

· 专题研究:肿瘤 ·

基于临床及MR影像特征评估直肠癌新辅助放化疗疗效的临床研究

孟慧慧^{1,2}, 余静¹, 吴飞云^{1*}

¹南京医科大学第一附属医院放射科, 江苏 南京 210029; ²南京医科大学附属逸夫医院放射科, 江苏 南京 211100

[摘要] 目的: 基于临床及磁共振成像影像特征, 探讨评估局部进展期直肠癌新辅助放化疗后病理完全缓解(pathological complete response, pCR)的危险因素。方法: 回顾性分析2014年12月—2022年11月经活检及临床诊断为局部进展期直肠癌且经过新辅助放化疗后行全直肠系膜切除的175例患者, 按7:3的比例随机分为训练组和验证组。训练组122例, 其中pCR组30例, 非完全病理缓解(non-pCR)组92例; 其余53例为验证组(pCR组10例, non-pCR组43例)。收集治疗前后患者的临床资料、影像检查及病理学数据。采用单因素、多因素Logistic回归分析局部进展期直肠癌新辅助治疗疗效。采用受试者工作特征(receiver operating characteristic, ROC)曲线评估预测因素的诊断效能, 计算曲线下面积(area under curve, AUC)、截断值、灵敏度、特异度, 并采用DeLong检验比较AUC值的差异。结果: 治疗前后肿块长径、治疗前后壁外深度、治疗后癌胚抗原值、治疗后肿块周围淋巴结状态、治疗前后壁外血管侵犯、治疗后的影像T分期及N分期、直肠系膜筋膜在pCR组和non-pCR组间差异有统计学意义, 经单因素及多因素Logistic回归分析发现, 治疗后壁外深度为评估新辅助放化疗疗效的独立危险因素。治疗后壁外深度在训练组和验证组中对预测新辅助放化疗疗效有较好的诊断效能。训练组和验证组的AUC值分别为0.783和0.765, 截断值分别为0.555和0.627, 灵敏度分别为0.870和0.852, 特异度分别为0.733和0.773。经Hosmer-Lemeshow拟合优度检验后差异无统计学意义。结论: 评估肿瘤侵犯壁外深度有助于评估局部进展期直肠癌新辅助放化疗后pCR率, 为临床提供了方便无创的诊断手段, 指导临床个体化治疗。

[关键词] 局部进展期直肠癌; 新辅助放化疗; 磁共振成像; 壁外深度

[中图分类号] R735.37

[文献标志码] A

[文章编号] 1007-4368(2025)04-443-10

doi: 10.7655/NYDXBNSN241039

Evaluate the efficacy of neoadjuvant chemoradiotherapy for locally advanced rectal cancer based on clinical and MR image data

MENG Huihui^{1,2}, YU Jing¹, WU Feiyun^{1*}

¹Department of Radiology, the First Affiliated Hospital of Nanjing Medical University, Nanjing 210029; ²Department of Radiology, Sir Runrun Hospital, Nanjing Medical University, Nanjing 211100, China

[Abstract] **Objective:** To explore the risk factors of pathological complete response (pCR) after neoadjuvant chemoradiotherapy in locally advanced rectal cancer based on clinical and magnetic resonance imaging (MRI) data. **Methods:** A retrospective analysis was conducted on 175 patients diagnosed with locally advanced rectal cancer through biopsy and clinical diagnosis from December 2014 to November 2022, who underwent total mesorectal excision (TME) after neoadjuvant chemoradiotherapy. These patients were randomly divided into a training set and a validation set in a 7:3 ratio. The training set included 122 patients, with 30 in the pCR group and 92 in the non-pCR group; the remaining 53 patients served as the validation set (10 in the pCR group and 43 in the non-pCR group). Clinical data, imaging examination and pathological data of patients before and after treatment were collected. Univariate and multivariate logistic regression analyses were used to evaluate the efficacy of neoadjuvant treatment in locally advanced rectal cancer. The diagnostic efficacy of predictive factors was evaluated by receiver operating characteristic (ROC) curve. The diagnostic efficacy of predictive factors was assessed using the receiver operating characteristic (ROC) curve, calculating the area under the curve (AUC), cut

[基金项目] 江苏省科教能力提升工程(JSDW202243)

*通信作者(Corresponding author), E-mail: wfy_njmu@163.com(ORCID: 0000-0002-3479-369X)

- off value, sensitivity, and specificity. Differences in AUC values were compared using the DeLong test. **Results:** Statistically significant differences were observed in the maximum tumor diameter before and after treatment, the depth of tumor infiltration before and after treatment, the CEA value after treatment, the number of lymph nodes around the tumor after treatment, extramural vascular invasion before and after treatment, imaging T and N stages after treatment, and the mesorectal fascia between the pCR and non-pCR groups. The univariate and multivariate logistic regression analysis identified extramural depth after treatment was an independent risk factor for evaluating the efficacy of neoadjuvant chemoradiotherapy. Extramural depth after treatment demonstrated good diagnostic efficacy in predicting the efficacy of neoadjuvant chemoradiotherapy in both the training and validation sets. The AUC values for the training and the validation sets were 0.783 and 0.765, respectively, with cutoff values of 0.555 and 0.627, sensitivity of 0.870 and 0.852, and the specificity of 0.733 and 0.773. There was no statistically difference after Hosmer-Lemeshow goodness of fit test. **Conclusion:** Evaluating the extramural depth is helpful to evaluate the pCR rate of locally advanced rectal cancer after neoadjuvant chemoradiotherapy in locally advanced rectal cancer, providing a convenient and non-invasive diagnostic tool for clinic practice and guiding individualized treatment.

[Key words] locally advanced rectal cancer; neoadjuvant chemoradiotherapy; magnetic resonance imaging; extramural depth

[J Nanjing Med Univ, 2025, 45(04): 443-452]

结直肠癌是世界范围内最常见的恶性肿瘤之一。最新全球癌症统计显示,结直肠癌发病率位居第3位(10%),死亡率为第2位(9.4%)^[1];中国、欧洲和北美新发结直肠癌病例占全球的50%以上^[2],其中直肠癌约占结直肠癌的39%。而在直肠癌中超过70%为局部进展期直肠癌(locally advanced rectal cancer, LARC)。LARC患者预后较差,对于这类患者,目前的标准治疗方式是新辅助放化疗(neoadjuvant chemoradiotherapy, nCRT)结束6周后行全直肠系膜切除术(total mesorectal excision, TME)^[3]。15%~30%的患者经过nCRT后可达到病理完全缓解(pathological complete response, pCR)^[4]。新的治疗策略提出对于经nCRT后临床完全缓解甚至达到pCR的患者可采用“等待-观察”策略,从而保留器官,避免重大手术,避免永久性结肠造口及相应并发症^[5-6]。由此可见,早期预测nCRT疗效有助于对患者进行分层治疗,减少患者治疗风险。

目前,磁共振成像(magnetic resonance imaging, MRI)因其良好的软组织分辨力在临床上被广泛应用于直肠癌的术前诊断。MRI可用于定位直肠癌肿块、测量肿块范围、判断肿块向周围结构的浸润、判断直肠癌的淋巴结转移及血管侵犯情况,对临床手术切除方式及范围具有较高的指导价值。T2加权成像(T2 weighted imaging, T2WI)可看到nCRT后病灶体积的缩小及纤维化改变。功能性MRI如弥散加权成像(diffusion-weighted imaging, DWI)、动态对比增强(dynamic contrast-enhanced magnetic resonance imaging, DCE-MRI)能反映肿瘤生长状态和生物学

特性以及组织内部血管密度和微循环灌注情况,从而评估nCRT的疗效^[7]。文献报道目前主要是经影像学数据或临床数据来评估预测LARC的nCRT后疗效,但影像数据项目较少^[8],结合多重影像数据及临床数据等综合因素以评估直肠癌nCRT疗效的研究也较少。为此,本研究基于临床及多重MRI影像特征,探讨LARC患者nCRT后pCR的影响因素。

1 对象和方法

1.1 对象

回顾性分析2014年12月—2022年11月南京医科大学第一附属医院经活检及临床诊断为LARC且经nCRT后行TME的175例患者,其中,男117例,女58例,年龄(22~82岁),平均(56.93±11.89)岁。pCR 40例,非病理完全缓解(non-pCR)者135例。

纳入标准:①经结肠镜取材活检病理确诊为原发直肠腺癌;②治疗前诊断为LARC(cT3~4/Nany, II~III期);③手术前接受完整nCRT治疗;④nCRT治疗前、后均接受MRI检查;⑤放化疗结束6~12周后行根治性手术治疗,并有明确的术后病理肿瘤退缩分级(tumor regression grade, TRG)。标准排除:①nCRT前接受其他抗肿瘤治疗;②不能耐受MRI检查或MRI图像质量欠佳;③临床资料或影像资料不完整;④未接受完整nCRT治疗;⑤未手术。本研究医院伦理委员会批准并知情同意。

1.2 方法

患者在nCRT前、nCRT后术前分别进行1次直肠MRI成像检查。检查使用3.0T MRI扫描仪

(MAGNETOM Verio, 西门子公司, 德国), 16通道骨盆相控阵线圈。扫描范围包括整个盆腔, 检查前患者禁食、禁水4~6 h。扫描序列和参数为: ①T2WI快速自旋回波序列, 包括矢状位、斜轴位(扫描平面垂直于病灶所在肠管的长轴)及冠状位, TR 4 550 ms, TE 99 ms, FOV 25 cm×25 cm, 矩阵768×768, 层厚3.0 mm, 层间距0.6 mm; ②DWI, 轴位扫描, TR 11 100 ms, TE 91 ms, FOV 25 cm×25 cm, 矩阵164×196, 层厚5.0 mm, 层间距0.5 mm, b值为0、1 000 s/mm²; ③增强T1WI, 轴位扫描, TR 1 080 ms, TE 9 ms, FOV 25 cm×25 cm, 矩阵290×320, 层厚3.0 mm, 层间距0.6 mm; 采用自动注射系统(Stellant MR注射系统)注射钆二胺造影剂(GE HealthCare公司, 美国)0.5 mol/L, 用量(mL)=体重(kg)×0.2 mL/kg, 流速2.5 mL/s。

1.2.1 治疗方案

所有患者术前均行直肠癌长程放化疗。放疗剂量: 每日剂量2 Gy, 每周5 d, 连续5周, 共25次, 总剂量50 Gy。同时, 患者口服卡培他滨化疗2个疗程, 剂量为1 000 mg/m², 每天2次。所有患者结束nCRT治疗后于6~12周行手术治疗, 遵循TME原则进行直肠癌根治术, 取得病理学诊断结果。

1.2.2 搜集患者资料

收集患者治疗前后的临床资料、影像检查数据。临床资料包括年龄、性别、nCRT时间及方式、癌胚抗原(carcinoembryonic antigen, CEA)及癌抗原CA19-9水平。从图像存档和通信系统检索导出图像, 记录患者影像检查数据, 包括肿块位置[低(0~5 cm)、中(5.1~10.0 cm)或高(10.1~15.0 cm)]、治疗前后肿块长径、肿块体积、肿块距肛缘距离、表观弥散系数(apparent diffusion coefficient, ADC)值、壁外深度(extramural depth, EMD)、MRI肿瘤T分期及N分期、系膜淋巴结及侧方淋巴结的数目与短径、治疗前后直肠系膜筋膜(mesorectal fascia, MF)、壁外血管侵犯(extramural vascular invasion, EMVI)。壁外深度即固有肌层外缘到肿瘤最外缘的距离, 测量时在斜轴位T2WI上取肿瘤浸润范围最大平面测量自固有肌层外缘到肿瘤最外缘的垂直距离, 注意与瘢痕或纤维组织相鉴别。MF与肿瘤之间距离≤1 mm称为MF受累, 记录为MF阳性, 否则为阴性。在MR上EMVI的迹象: ①在血管结构内存在肿瘤信号强度; ②血管扩张; ③肿瘤扩张到达或超出血管壁, 破坏血管边界。

由1名具有3年及1名具有10年MRI影像诊断经验的医师对图像进行分析。定量特征测量值由

2名医生分别测量, 相差控制在10%以内, 取平均值作为结果。定性特征对有异议的结果由医师讨论意见一致后作为结论。

1.2.3 肿瘤退缩分级及病理评估

为评估肿瘤nCRT疗效, 根据美国癌症联合委员会(American Joint Committee on Cancer, AJCC)第8版TRG评分系统, 评估患者病理肿瘤退缩分级: 0级(完全退缩)为镜下无肿瘤细胞; 1级(接近完全退缩)指镜下仅单细胞或小癌细胞群残留; 2级(部分退缩)是肿瘤残留但少于纤维化间质; 3级(退缩不良或无退缩)指无或极少肿瘤细胞坏死^[9]。本研究将pTRG 0级定义为nCRT后pCR组, pTRG 1、2和3级被定义为non-pCR组。病例数据搜集如图1、2。

1.3 统计学方法

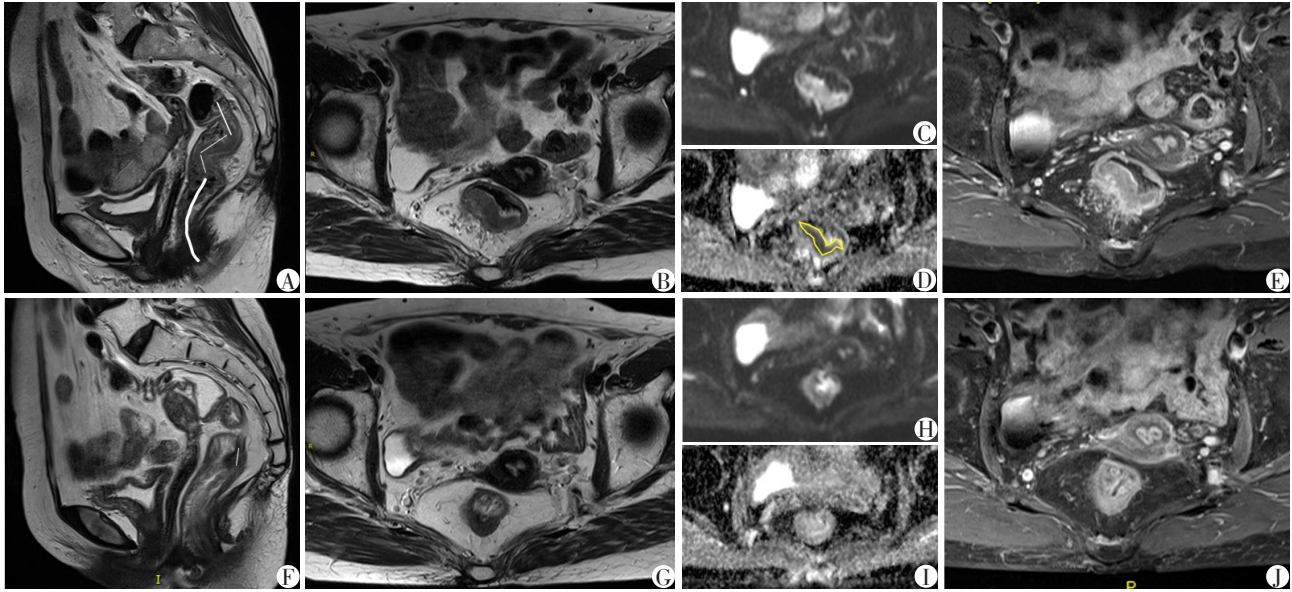
采用SPSS 26.0软件进行统计学分析。采用Kappa分析法对2位阅片者评分一致性进行检验。Shapiro-Wilk检验定量资料是否符合正态分布, 符合正态分布的计量资料以均数±标准差($\bar{x} \pm s$)表示, 独立样本 t 检验; 偏态分布数据以中位数(四分位数)[$M(P_{25}, P_{75})$]表示, 采用Kruskal-Wallis秩和检验。计数资料以频数(百分比)表示, 组间比较采用 χ^2 检验或Fisher精确检验。采用单因素、多因素Logistic回归分析筛选LARC新辅助治疗疗效预测因子。以病理学结果为“金标准”, 采用受试者工作特征(receiver operating characteristic, ROC)曲线评估预测因素的诊断效能。将患者按7:3比例随机分为训练组、验证组, 对模型进行验证, 计算曲线下面积(area under curve, AUC)、截断值、灵敏度、特异度, 并采用DeLong检验比较AUC值的差异。 $P < 0.05$ 为差异有统计学意义。

2 结果

2.1 临床特点

本研究共纳入175例LARC患者, 其中, 男117例, 女58例, 年龄为(56.93±11.89)岁; pCR组40例(22.9%), non-pCR组135例(77.1%)。训练组患者122例(pCR组30例, non-pCR组92例), 验证组患者53例(pCR组10例, non-pCR组43例)。两位阅片者一致性较好, Kappa值为0.825(95% CI: 0.763~0.905)。训练组和验证组之间疗效分组及临床特征差异均无统计学意义(表1、2)。

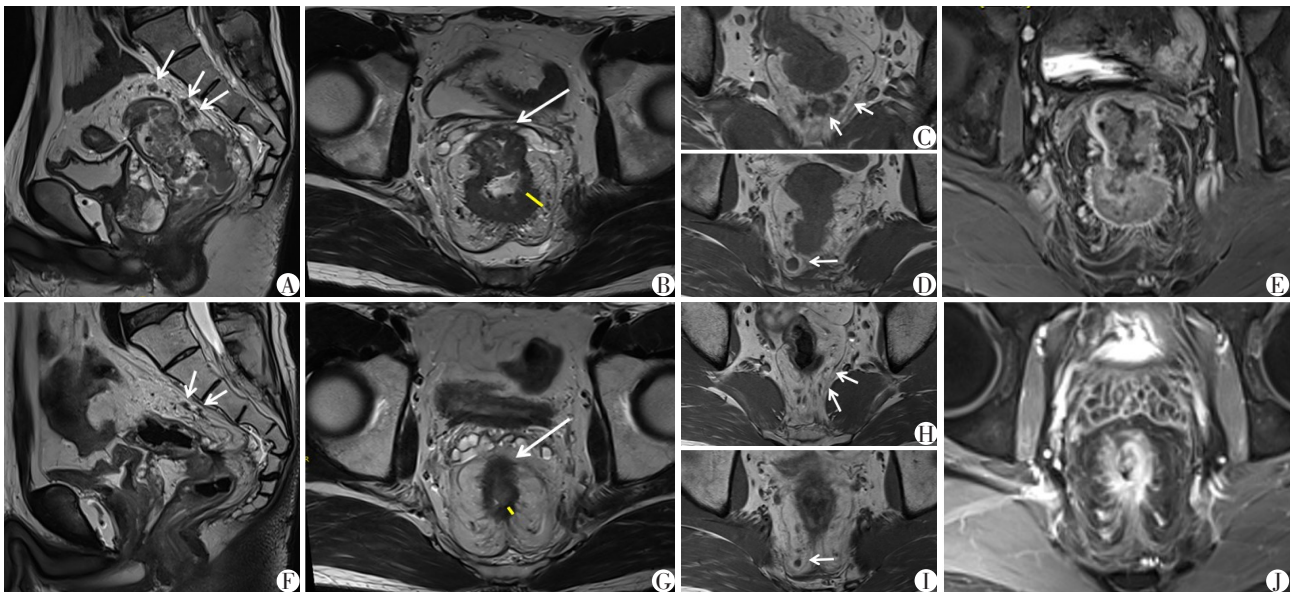
训练组和验证组在pCR组和non-pCR组间部分临床特征(治疗前后肿块长径、治疗前后壁外深度、治疗后CEA值、治疗后肿块周围淋巴结数、治疗前



A 62-year-old female with locally advanced rectal cancer underwent surgery. Pathology showed mucosal defects with granulation tissue, fibrous tissue growth, and infiltration of acute and chronic inflammatory cells, but no tumor cells were found. TRG score: Grade 0. MR images before nCRT (sagittal T2WI, transverse T2WI, DWI, ADC, and DCE-MRI) are shown in A–E. MR images after nCRT are shown in F–J. In figure A, the thin white line measures tumor length and the thick white line measures the distance from the tumor to the anal margin. Figure D shows the ADC value of the tumor, measured using T2WI, DWI, and DCE-MRI. The thin white line in figure F shows the tumor length after treatment.

图1 pCR患者nCRT前后MR图像

Figure 1 MR images of the pCR patient before and after nCRT



A 49-year-old male patient with locally advanced rectal cancer. After operation, under the pathological microscope, multifocal mucus lakes were formed in the fibrous connective tissue outside the mucosal layer to the muscularis propria, and only a few adenocarcinoma tissues were seen in it. Stage after neoadjuvant chemotherapy (YPTNM): YP T3N0Mx, TRG score: Grade 1. Figures A–E show the pre-treatment MR images (sagittal T2WI, transverse T2WI, axial T1WI, and DCE-MRI), and figures F–J show the post-treatment MR images. Brief arrows in figures A, C, D, F, H, and I indicate lymph nodes around the tumor before and after treatment. In figures B and G, the long arrow shows tumor invasion of the mesorectal fascia (MF positive), and the yellow line measures the depth of tumor invasion, from the outer edge of the muscularis propria to the outermost edge of the tumor.

图2 non-pCR患者nCRT前后MR图像

Figure 2 MR images of the non-pCR patient before and after nCRT

后EMVI和治疗后的MRI肿瘤T分期、N分期、MF) 差异有统计学意义($P < 0.05$,表3、4)。

2.2 Logistic回归分析

对训练组临床特征进行单因素Logistic回归分析

表1 训练组和验证组的临床及病理资料

Table 1 Clinical and pathological data of training and validation sets

Variable	Training set(n=122)	Validation set(n=53)	$t/\chi^2/Z$	<i>P</i>
Age(years, $\bar{x} \pm s$)	56.34 ± 12.15	58.26 ± 11.26	0.982	0.328
Sex[n(%)]			0.457	0.499
Male	84(68.9)	33(62.3)		
Female	38(31.1)	20(37.7)		
nCRT effect[n(%)]			0.686	0.407
pCR set	30(24.6)	10(18.9)		
non-pCR set	92(75.4)	43(81.1)		
Tumor location[n(%)]			0.054	0.157
Upper	18(14.8)	11(20.8)		
Middle	86(70.5)	30(56.6)		
Lower	18(14.8)	12(22.6)		
Tumor length[cm, $M(P_{25}, P_{75})$]				
Pre	4.80(1.80, 10.80)	4.80(2.70, 10.20)	-1.420	0.157
Post	3.30(0, 10.30)	3.10(0, 8.40)	-0.401	0.689
CEA[ng/mL, $M(P_{25}, P_{75})$]				
Pre	7.24(0.87, 357.30)	5.60(1.39, 75.36)	-1.819	0.071
Post	2.36(0.41, 149.50)	2.49(0.81, 23.15)	-0.741	0.460

表2 训练组和验证组的影像学资料

Table 2 Imaging data of training and validation sets

Variable	Training set(n=122)	Validation set(n=53)	$t/\chi^2/Z$	<i>P</i>
Pre-T[n(%)]			0.437	0.804
T2	1(0.8)	0(0)		
T3	89(73.0)	39(73.6)		
T4	32(26.2)	14(26.4)		
Post-T[n(%)]			5.271	0.153
T1	1(0.8)	3(5.7)		
T2	33(27.0)	12(22.6)		
T3	80(65.6)	32(60.4)		
T4	8(6.6)	6(11.3)		
Pre-N[n(%)]			1.642	0.440
N0	13(10.7)	4(7.5)		
N1	68(55.7)	35(66.0)		
N2	41(33.6)	14(26.4)		
Post-N[n(%)]			0.860	0.651
N0	59(48.4)	26(49.1)		
N1	51(41.8)	24(45.3)		
N2	12(9.8)	3(5.7)		
EMD[cm, $M(P_{25}, P_{75})$]				
pre	0.60(0, 4.90)	0.40(0.10, 3.30)	-1.182	0.239
post	0.33(0, 1.80)	0.40(0, 2.10)	-1.286	0.200
Pre-MF[n(%)]			3.595	0.058
+	65(53.3)	14(26.4)		
-	57(46.7)	39(73.6)		
Pre-EMVI[n(%)]			0.006	0.939
+	43(35.2)	19(35.8)		
-	79(64.8)	34(64.2)		
LN count around tumor[$M(P_{25}, P_{75})$]				
Pre	2.0(1.0, 5.0)	2.0(1.0, 4.0)	0.772	0.379
Post	1.0(0, 2.0)	0(0, 1.0)	8.953	0.069

后发现:治疗后肿块长径、治疗前MF、治疗后壁外深度及治疗后肿块周围淋巴结数与nCRT疗效相关($P < 0.05$),多因素Logistic回归分析显示治疗后壁外深度

是nCRT疗效的独立危险因素($P=0.003$,表5、6)。

2.3 预测模型评估

治疗后壁外深度在训练组和验证组中对预测

表3 训练组nCRT后pCR组及non-pCR组特征比较
Table 3 Comparison of characteristics between pCR and non-pCR groups in the training set after nCRT

Variable	Training set($n=122$)		$t/\chi^2/Z$	P
	pCR group($n=30$)	non-pCR group($n=92$)		
Age(years, $\bar{x} \pm s$)	55.53 \pm 10.66	56.61 \pm 12.64	-0.420	0.676
Sex[$n(\%)$]			0.958	0.328
Male	18(60.0)	66(71.7)		
Female	12(40.0)	26(28.3)		
Tumor location[$n(\%)$]			0.931	0.628
Upper	3(10.0)	15(16.3)		
Middle	23(76.7)	63(68.5)		
Lower	4(13.3)	14(15.2)		
Tumor length[cm, $M(P_{25}, P_{75})$]				
Pre	4.60(4.30, 5.60)	4.90(4.30, 5.50)	-1.923	0.057
Post	2.70(2.00, 3.15)	3.30(2.30, 3.90)	-2.607	0.010
Pre-T[$n(\%)$]			2.666	0.264
T2	0(0)	1(1.1)		
T3	25(83.3)	64(69.6)		
T4	5(16.7)	27(29.3)		
Post-T[$n(\%)$]			41.991	<0.001
T1	1(3.3)	0(0)		
T2	21(70.0)	12(13.0)		
T3	8(26.7)	72(78.3)		
T4	0(0)	8(8.7)		
Pre-N[$n(\%)$]			0.001	0.969
N0	3(10.0)	10(10.9)		
N1	17(56.7)	51(55.4)		
N2	10(33.3)	31(33.7)		
Post-N[$n(\%)$]			2.995	0.084
N0	18(60.0)	41(44.6)		
N1	11(21.6)	40(43.5)		
N2	1(3.3)	11(12.0)		
EMD[cm, $M(P_{25}, P_{75})$]				
Pre	0.59(0.23, 0.55)	0.60(0.33, 0.86)	-2.182	0.031
Post	0(0, 0.40)	0.40(0.20, 0.60)	-4.271	<0.001
Pre-MF[$n(\%)$]			2.155	0.142
+	12(40.0)	39(42.4)		
-	18(60.0)	53(57.6)		
Pre-EMVI[$n(\%)$]			12.625	<0.001
+	2(6.7)	41(44.6)		
-	28(93.3)	51(55.4)		
LN count around tumor[$M(P_{25}, P_{75})$]				
Pre	2.0(1.0, 5.0)	2.0(1.0, 5.0)	0.250	0.617
Post	0(0, 1.0)	1.0(0, 2.0)	4.839	0.028
CEA[ng/mL, $M(P_{25}, P_{75})$]				
Pre	7.40(2.68, 14.88)	6.76(2.86, 19.90)	1.005	0.323
Post	2.06(1.36, 2.99)	2.62(1.86, 4.12)	-1.111	0.269

表4 验证组 nCRT 后 pCR 组及 non-pCR 组特征比较
Table 4 Comparison of characteristics between pCR and non-pCR groups in the validation set after nCRT

Variable	Validation set(n=53)		$t/\chi^2/Z$	P
	pCR group(n=10)	non-pCR group(n=43)		
Age(years, $\bar{x} \pm s$)	60.10 ± 12.22	57.84 ± 11.13	0.569	0.572
Sex[n(%)]			0.027	0.870
Male	6(60.0)	27(26.8)		
Female	4(40.0)	16(16.2)		
Tumor location[n(%)]			1.114	0.572
Upper	2(20.0)	9(20.9)		
Middle	7(70.0)	23(53.5)		
Lower	1(10.0)	11(25.6)		
Tumor length[cm, $M(P_{25}, P_{75})$]				
Pre	4.50(3.45, 5.10)	4.50(4.05, 5.20)	-1.184	0.855
Post	3.05(2.35, 4.15)	3.50(2.70, 4.45)	-1.708	0.094
Pre-T[n(%)]			1.097	0.295
T2	0(0)	0(0)		
T3	6(60.0)	33(76.7)		
T4	4(40.0)	10(23.3)		
Post-T[n(%)]			7.425	0.032
T1	2(20.0)	1(2.3)		
T2	4(40.0)	8(18.6)		
T3	3(30.0)	29(67.4)		
T4	1(10.0)	5(11.6)		
Pre-N[n(%)]			2.431	0.300
N0	0(0)	4(9.3)		
N1	9(90.0)	26(60.5)		
N2	1(10.0)	13(30.2)		
Post-N[n(%)]			4.137	0.130
N0	8(80.0)	18(41.9)		
N1	2(20.0)	22(51.2)		
N2	0(0)	3(7.0)		
EMD[cm, $M(P_{25}, P_{75})$]				
Pre	0.40(0.25, 0.60)	0.50(0.34, 0.80)	-1.204	0.234
Post	0(0, 0.40)	0.40(0.25, 0.60)	-0.798	0.429
Pre-MF[n(%)]			0.467	0.494
+	4(40.0)	10(23.3)		
-	6(60.0)	33(76.7)		
Pre-EMVI[n(%)]			0.631	0.427
+	2(20.0)	17(39.5)		
-	8(80.0)	26(60.5)		
LN count around tumor[$M(P_{25}, P_{75})$]				
Pre	1.5(1.0, 3.0)	2.0(1.0, 4.0)	0.996	0.318
Post	0(0, 0)	1.0(0, 2.0)	5.523	0.019
CEA[ng/mL, $M(P_{25}, P_{75})$]				
Pre	9.34(1.90, 19.79)	5.00(2.80, 11.03)	0.914	0.365
Post	2.24(1.50, 3.50)	2.54(1.60, 3.65)	-0.807	0.424

nCRT 疗效有较好的诊断效能。训练组和验证组的 AUC 值分别为 0.783 和 0.765, 截断值分别为 0.555 和 0.627, 灵敏度分别为 0.870 和 0.852 以及特

异度分别为 0.733 和 0.773(图 3)。经 Hosmer-Lemeshow 拟合优度检验后均无统计学差异(训练组及验证组的 P 值分别为 0.659、0.350), 显示曲线未偏

表5 nCRT疗效预测影响因素的单因素 Logistic 回归分析
Table 5 Univariate logistic regression analysis of factors influencing the prediction of nCRT efficacy

Variable	Univariate logistic regression analysis	
	OR(95%CI)	P
Age	1.007(0.974-1.042)	0.673
Sex	1.692(0.716-3.999)	0.231
Tumor location	0.861(0.403-1.841)	0.699
Tumor length(cm)		
Pre	1.374(0.984-1.917)	0.062
Post	1.743(1.139-2.666)	0.010
T		
Pre	1.836(0.683-4.936)	0.229
Post	16.315(6.017-44.239)	<0.001
N		
Pre	0.987(0.510-1.910)	0.969
Post	1.831(0.917-3.658)	0.086
EMD(cm)		
Pre	1.792(0.758-4.236)	0.184
Post	57.010(7.115-456.780)	<0.001
Pre-MF	5.225(1.688-16.178)	0.004
Pre-EMVI	11.255(2.531-50.054)	0.001
LN count around tumor		
Pre	1.069(0.925-1.237)	0.365
Post	1.546(1.086-2.200)	0.016
CEA(ng/mL)		
Pre	0.993(0.983-1.003)	0.170
Post	1.449(1.033-2.033)	0.032

离拟合。

3 讨论

目前,临床研究中常用于 LARC 新辅助治疗效果预测的因子主要为临床特征、生物学标志物和影

表6 nCRT疗效预测影响因素的多因素 Logistic 回归分析
Table 6 Multivariate logistic regression analysis of factors influencing the prediction of nCRT efficacy

Variable	Multivariate logistic regression analysis	
	OR(95%CI)	P
Post-tumor length(cm)	1.425(0.962-2.111)	0.077
Post-T	NA	NA
Post-EMD(cm)	9.885(2.136-45.734)	0.003
Pre-MF	0.535(0.226-1.267)	0.155
Pre-EMVI	NA	NA
Post-LN count around tumor	1.400(0.969-2.023)	0.073

OR: odds ratio; NA: not included in the variable.

像学标志物^[8-9],本研究综合考虑并研究了这些预测因素,通过单因素及多因素 Logistic 回归分析表明,治疗后肿瘤壁外深度是 nCRT 后出现 pCR 的直肠癌患者的独立预测因素,在单因素及多因素 Logistic 回归分析中,治疗后肿瘤壁外深度 OR 值较高, P 均 < 0.05。当治疗后壁外深度明显减小时,能有效预测 nCRT 疗效,可协助临床制定治疗方案,实现为患者个体化诊疗。

60%~70%的直肠癌患者在最初诊断时被分类为 T3 期,他们的 5 年生存率从 30%~80% 不等,美国国立综合癌症网络(National Comprehensive Cancer Network, NCCN)临床实践指南建议所有 T3 期直肠癌患者均进行 nCRT,这已被越来越多的研究质疑其合理性。因此,区分将受益于 nCRT 的高风险 T3 期患者以及适合接受直接手术的低风险 T3 期患者是个体化医学的关键。肿瘤壁外深度已被证明是 LARC 局部复发的独立预测因素^[10]。已有多项研究结果显示,肿瘤的 T3 亚阶段分期及肿瘤侵犯的壁外

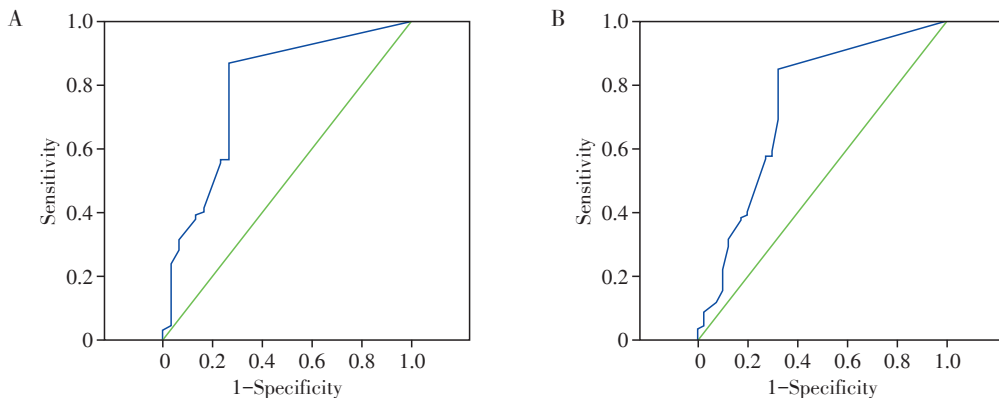


图3 训练组(A)和验证组(B)治疗后壁外深度预测 nCRT 疗效的 ROC 曲线

Figure 3 ROC curves for predicting the effectiveness of nCRT based on extramural depth after treatment in the training group (A) and validation group(B)

深度有助于预测LARC患者对nCRT的肿瘤反应及生存率^[11-12], 这些与本研究结果一致。

在早期的研究中, Reggiani等^[13]揭示, 肿瘤长径>3 cm是一项独立预后因素, 提示患者具有更短的无病生存期(disease-free survival, DFS)和更低的肿瘤特异性生存率(cancer-specific survival, CSS)。Jankowski等^[14]认为, 若患者肿瘤长径>7 cm, 则不应选择观察和等待策略。本研究单因素Logistic回归分析中, 治疗后肿块长径与nCRT疗效明显相关, 但是在多因素Logistic回归分析中, 治疗后肿块长径并非独立预测因素, 可能是由于治疗后肿瘤壁外深度与直肠癌nCRT疗效关联更加紧密, 从而导致在多因素Logistic回归分析中治疗后肿块长径预测效果不显著。另有研究表明, 肿瘤长度不能全面反映肿瘤的特征并证实肿瘤体积在预测肿瘤预后中具有较高的价值。Lutsyk等^[15]发现, 在187例LARC患者中, 肿瘤体积<39.5 cm³是pCR的重要预测因素。类似地, Yang等^[16]在对412例接受nCRT的患者的研究中证明肿瘤体积<37.3 cm³可以预测pCR。然而在本研究中肿瘤体积与nCRT疗效无明显相关, 可能与本研究中大部分患者在nCRT后皆疗效较好并均产生明显肿瘤体积退缩有关。

EMVI被定义为在固有肌层以外的内皮细胞内衬血管内存在恶性细胞。多项研究表明, EMVI与nCRT直肠癌患者的DFS有显著相关性。Sakanaka等^[17]研究表明, 在评估直肠癌nCRT疗效中, MR-EMVI的灵敏度和特异度分别为90.48%和41.14%。在本研究中, 治疗前EMVI亦具有统计学意义($P < 0.001$), 但壁外血管侵犯被定义为在固有肌层以外的内皮细胞内衬血管内存在恶性细胞, 以病理镜下观察为准; 而在MR影像中仅在DWI上看到明显异常血管内高信号或粗大不规则血管信号影方可诊断为EMVI阳性, 考虑到影像上诊断EMVI阳性较病理明显滞后, 不能反映病例真实血管侵犯状态, 故Logistic回归分析中未纳入此项结果。

多项研究表明, 直肠癌的T、N分期对于nCRT疗效有较高的评估作用。肿瘤的TNM分期、淋巴结等可以作为预测肠癌预后的重要依据^[18]。有文章显示nCRT治疗后MRI肿瘤T分期($\kappa=0.157$)、淋巴结分期($\kappa=0.138$)和环周切缘($\kappa=0.138$)和病理之间的一致性较差^[19], 这与本研究结论相一致, 可能与Logistic回归分析中差异不显著有关。

目前部分文献发现, nCRT治疗前CEA水平较低可作为预测pCR的指标^[20]。然而本研究结果显

示, pCR患者中nCRT前CEA水平在正常范围内的患者所占比例约为60.2%、non-pCR者约为53.2%, 二者的差异不具统计学意义。

本研究的局限性与不足在于: ①研究结果来自于单一机构, 需要多中心验证; ②在标准的选择下, 纳入的病例仍旧较少; ③研究为回顾性研究, 可能存在选择性偏倚; ④本研究证实了肿瘤浸润壁外深度是评估LARC的独立预测因素, 其在临床上的应用及意义仍需后续进一步研究。

综上, 评估肿瘤侵犯壁外深度有助于评估LARC nCRT后pCR率, 可有效评估直肠癌nCRT疗效, 可作为nCRT疗效的评价指标, 并指导临床进行个体化治疗。

利益冲突声明:

所有作者声明无利益冲突。

Conflict of Interests:

All of the authors have no conflict of interests to declare.

作者贡献声明:

吴飞云设计本研究的方案, 对文章进行最终修改; 孟慧慧搜集数据、起草和撰写稿件, 获取、分析和解释本研究的数据; 余静修改、润色稿件, 按编辑部的修改意见对稿件进行核修, 对学术问题进行解答; 所有作者都同意发表最终修改稿, 同意对研究工作各方面的诚信问题负责。

Author's Contributions:

WU Feiyun designed the study protocol and made the final revisions to the manuscript. MENG Huihui collected data, drafted and wrote the manuscript, and obtained, analyzed, and interpreted the data for this study. YU Jing revised and polished the manuscript, made revisions according to the editorial comments, and addressed academic issues. All authors agree to publish the final revised draft and to be responsible for the integrity of all aspects of the research work.

[参考文献]

- [1] BRAY F, LAVERSANNE M, SUNG H, et al. Global cancer statistics 2022: GLOBOCAN estimates of incidence and mortality worldwide for 36 cancers in 185 countries[J]. CA Cancer J Clin, 2024, 74(3): 229-263
- [2] LI N, LU B, LUO C Y, et al. Incidence, mortality, survival, risk factor and screening of colorectal cancer: a comparison among China, Europe, and Northern America[J]. Cancer Lett, 2021, 52(2): 255-268
- [3] ORONSKY B, REID T, LARSON C, et al. Locally advanced rectal cancer: the past, present, and future[J]. Semin Oncol, 2020, 47(1): 85-92
- [4] WILLIAMS H, OMER M D, THOMPSON M H, et al. MRI predicts residual disease and outcomes in watch-and-wait patients with rectal cancer[J]. Radiology, 2024, 312(3):

- e232748
- [5] ELHOMSI M, BERCE A, CHAHWAN S, et al. Watch & wait - post neoadjuvant imaging for rectal cancer[J]. *Clin Imaging*, 2024, 110: 110166
- [6] MIRANDA J, ANDRIEU C P, NINCEVIC J, et al. Advances in MRI-based assessment of rectal cancer post-neoadjuvant therapy: a comprehensive review [J]. *J Clin Med*, 2023, 13(1): 172
- [7] XIA Y R, LI S, WANG H Z, et al. MRI-based radiomics to predict neoadjuvant chemoradiotherapy outcomes in locally advanced rectal cancer: a multicenter study[J]. *Clin Transl Radiat Oncol*, 2023, 38: 175-182
- [8] 李华秀, 李振辉, 李 鹏, 等. CT影像组学预测局部进展期直肠癌新辅助治疗的效果[J]. *中国医学影像学杂志*, 2020, 28(1): 44-50
LI H X, LI Z H, LI K, et al. Predicting the effect of neoadjuvant therapy for locally advanced rectal cancer by CTRadiomics [J]. *Chinese Journal of Medical Imaging*, 2020, 28(1): 44-50
- [9] ATTHAPHORN T, MITHAT G, JINRU S, et al. Comparison of tumor regression grade systems for locally advanced rectal cancer after multimodality treatment [J]. *J Natl Cancer Inst*, 2014, 106(10): dju248
- [10] ZHANG X Y, LI X T, SHI Y J, et al. Correlation between the distance to mesorectal fascia and prognosis of cT3 rectal cancer: results of a multicenter study from China [J]. *Dis Colon Rectum*, 2022, 65(3): 322-332
- [11] LU Z H, XIA K J, JIANG H, et al. Textural differences based on apparent diffusion coefficient maps for discriminating pT3 subclasses of rectal adenocarcinoma [J]. *World J Clin Cases*, 2021, 9(24): 6987-6998
- [12] LIU Q, ZANG Y, ZHOU D, et al. The importance of preoperative T3 stage substaging by 3D endorectal ultrasonography for the prognosis of middle and low rectal cancer [J]. *J Clin Ultrasound*, 2024, 52(3): 249-254
- [13] LUCA B R, SIMONA L, FEDERICA D, et al. Do pathological variables have prognostic significance in rectal adenocarcinoma treated with neoadjuvant chemoradiotherapy and surgery? [J]. *World J Gastroenterol*, 2017, 23(8): 1412-1423
- [14] MICHAL J, LUCYNA P, MACIEJ R, et al. Watch-and-wait strategy in rectal cancers: is there a tumour size limit? Results from two pooled prospective studies [J]. *Radiother Oncol*, 2021, 160: 229-235
- [15] LUTSYK M, AWAWDA M, GOUREVICH K, et al. Tumor volume as predictor of pathologic complete response following neoadjuvant chemoradiation in locally advanced rectal cancer [J]. *Am J Clin Oncol*, 2021, 44(9): 482-486
- [16] YANG F, HILL J, ABRAHAM A, et al. Tumor volume predicts for pathologic complete response in rectal cancer patients treated with neoadjuvant chemoradiation [J]. *Am J Clin Oncol*, 2022, 45(10): 405-409
- [17] SAKANAKA T, IWAMOTO H, MATSUDA K, et al. Double negativity of MRI-detected and pathologically-diagnosed extramural venous invasion is a favorable prognostic factor for rectal cancer [J]. *Ann Surg Oncol*, 2024, 31(4): 2425-2438
- [18] 付志强, 高启行, 郭文文, 等. 结肠癌中 ALOX12 表达与临床病理特征及预后的关系分析 [J]. *南京医科大学学报(自然科学版)*, 2024, 44(5): 643-648
FU Z Q, GAO Q X, GUO W W, et al. Analysis of the relationship between ALOX12 expression and clinicopathological features and prognosis in colon cancer [J]. *Journal of Nanjing Medical University (Natural Sciences)*, 2024, 44(5): 643-648
- [19] AKGÜL Ö, MARTLI H F, GÖKTAS A, et al. Comparison of preoperative magnetic resonance imaging with postoperative pathology results in rectal cancer patients undergoing neoadjuvant therapy [J]. *ANZ J Surg*, 2024, 94(6): 1133-1137
- [20] WANG Y, PAN Z, LI S, et al. Prediction and validation of pathologic complete response for locally advanced rectal cancer under neoadjuvant chemoradiotherapy based on a novel predictor using interpretable machine learning [J]. *Eur J Surg Oncol*, 2024, 50(12): 108738

[收稿日期] 2024-10-09

(本文编辑: 唐 震)